J Fluoresc (2015) 25:1297–1302
DOI 10.1007/s10895-015-1617-y

ORIGINAL ARTICLE

A Novel Naphthalene-Immobilized Nanoporous SBA-15 as a Highly Selective Optical Sensor for Detection of Fe^{3+} in Water

Mehdi karimi[1] · **Alireza Badiei**[1,2] · **Ghodsi Mohammadi Ziarani**[3]

Received: 28 March 2015 / Accepted: 5 July 2015 / Published online: 25 July 2015

Abstract A novel organic-inorganic hybrid optical sensor (SBA-NCO) was designed and synthesized through immobilization of isocyanatopropyl-triethoxysilane and 1-aminonaphthalene onto the surface of SBA-15 by post-grafting method. The characterization of materials using XRD, TEM, N_2 adsorption-desorption, and FT-IR techniques confirmed the successful attachment of organic moieties and preserving original structure of SBA-15 after modification step. Fluorescence experiments demonstrated that SBA-NCO was a highly selective optical sensor for the detection of Fe^{3+} directly in water over a wide range of metal cations including Na^+, Mg^{2+}, Al^{3+}, K^+, Ca^{2+}, Cr^{3+}, Mn^{2+}, Fe^{2+}, Co^{2+}, Ni^{2+}, Cu^{2+}, Zn^{2+}, Cd^{2+}, Hg^{2+}, and Pb^{2+} in a wide pH values.

Keywords SBA-15 · Optical sensor · Fe^{3+} · Naphthalene · Fluorescence · Nanoporous silica

Introduction

In recent years, the fluorescent sensors as a powerful optical analytical technique for the detection of low level of various analytes such as anions and metal cations have been progressively developed due to the simplicity, portability, cost effective and selectivity for monitoring specific analyte in environmental and biological systems [1–4]. Among various ions, Fe^{3+} is one of the most investigated analyte in the field of fluorescent sensor [5, 6] because it is an abundant essential ion in biological system and plays crucial rules in living organism activities, typically in the storage and transport of oxygen to tissues. However, both its deficiency and excess accumulation are associated to the various disorders such as anemia, damage to the liver and kidney and Alzheimer's and Parkinson's diseases [7–10]. Indeed, there are very promising Fe^{3+}-fluorescent sensor which were prepared in a simple procedure and were able to detect this ion in trace amount [11–14]. Since Fe^{3+} is mostly occurred in aqueous media, it is of great importance that the sensor be able of on-line detection of this ion directly in water. To days, most of the reported Fe^{3+}-fluorescent sensors required organic solvents for optimal performance, for example DMF [15, 16], methanol [17, 18], acetonitrile [19, 20], and THF [21], which limited their direct applicability in pure water, Thus, there is still room for the development of new class of fluorescent sensors for Fe^{3+} to overcome this shortage.

Very recently, covalent immobilization of fluorophore groups onto the inorganic nanomaterial substrates, as organic-inorganic hybrid optical sensor, have been introduced into the fluorescent sensor field. Among various nanomaterials, nanoporous silica materials have recently become the first nominate for preparing hybrid optical sensors because they offer large pore size, hydrothermal stability, and simple and rapid approach in monitoring analytes due to the their uniform channels with high specific surface area [22–28]. The presence of abundant OH active groups on the surface of silica nanomaterials and availability of various organosilica functionalities, as a linker, permit the attachment of a wide variety of fluorophores onto their surface. In

✉ Alireza Badiei
abadiei@khayam.ut.ac.ir

[1] School of Chemistry, College of Science, University of Tehran, Tehran, Iran

[2] Nanobiomedicine Center of Excellence, Nanoscience and Nanotechnology Research Center, University of Tehran, Tehran, Iran

[3] Department of Chemistry, Faculty of Science, Alzahra University, Tehran, Iran

particular, SBA-15, a two-dimensional hexagonal arrangement of cylindrical pores, is a promising one to be used as inorganic support owing to tunable and larger pore sizes facilitating diffusion of analytes through channels. In addition, higher hydrothermal stability of SBA-15 makes it a durable support in various aqueous environment with varied pH without collapsing in structure. Moreover, since both water and organic solvent can diffuse into the channel of nanoporous silica materials, the solubility properties of grafted fluorophores become solvent independent, thereby, hybrid optical sensor based on SBA-15 can be directly applied in aqueous media even if it contains water insoluble fluorophores.

In this sense and as a part of our continuing interest in the development of optical sensors for Fe^{3+} [29, 30], a naphthalene derivative as flourophore was covalently grafted onto the SAB-15 surface via 3-isocyanatopropyl-triethoxysilane as a linker for preparing a novel selective and sensitive hybrid optical sensor for the detection of Fe^{3+}. In this system, the urea unit acted as a binding site for absorbing Fe^{3+} ions.

Materials and Instruments

Tetraethylorthosilicate (TEOS), pluronic P123, hydrochloric acid 35 %, tetrahydrofuran (THF), 3-isocyanatopropyl-triethoxysilane, 1-amino-naphthlene, Metal nitrate salts (except for $FeSO_4$). All above materials were used without any further purification. The deionized water was used in all procedures. Low-angle X-ray scattering measurements were performed on an X'Pert Pro MPD diffractometer using Cu K_α radiation (λ=1.5418 Å). N_2 adsorption-desorption isotherms were obtained using BELSORP-miniII instrument at liquid nitrogen temperature (−196 °C). All samples were degassed at 100 °C before performing measurements. The Brunauer-Emmet-Teller (BET) and Barrett-Joyner-Halenda (BJH) equations were applied on sorption data using BELSORP analysis software to calculate physical properties of materials such as specific surface area, pore diameter, pore volume and pore size distribution. The Fourier transform infrared (FT-IR) spectra of samples were recorded on a RAYLEIGH WQF-510A apparatus. Transmission electron microscopy (TEM) was performed on Zeiss EM900 instrument at an accelerating voltage of 80 kV. Samples were dispersed in ethanol using an ultrasonic bath and a drop of the ethanol mixture was placed on a lacey carbon-coated copper grid for analysis. Thermogravimetric analysis (TGA) was carried out in a TGA Q50 V6.3 Build 189 instrument from ambient temperature to 1000 °C with a ramp rate of 20 °C/min in air. Fluorescence spectra were recorded on Agilent G980A instrument.

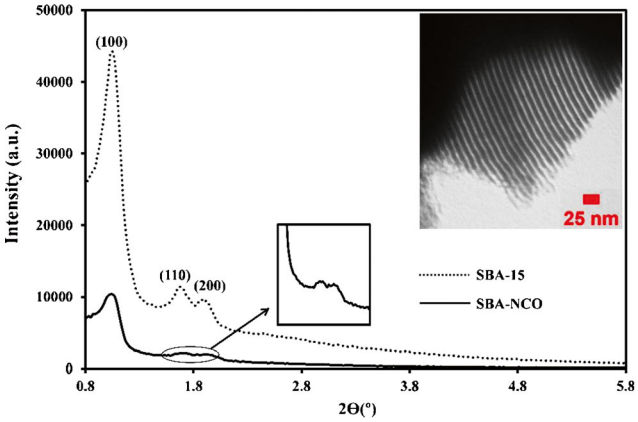

Fig. 1 Low angle powder XRD patterns of (a) SBA-15 and (b) SBA-NCO (inset: TEM image of SBA-15)

Preparation of SBA-15

SBA-15 was prepared based on Ref [31]. A homogenous solution of 11.7 g Pluronic P123, 303.4 g water, 73.3 g HCl 37 % was prepared followed by stirring for 3 h at 55 °C. Next, 25 g TEOS was added under stirring and solution was remained at static condition for 24 h at 55 °C. Afterwards, the reaction batch was kept in oven for another 24 h at 100 °C. The product was washed with HCl/ethanol mixture and finally calcined under air for 3 h at 550 °C.

Preparation of SBA-NCO

In a typical procedure, 5 mmol 3-isocyanatopropyl-triethoxysilane and 5 mmol 1-amino-naphthalene was dissolved in 50 ml THF and refluxed for 6 h. Then, 1 g SBA-15 was added to the container and mixture was refluxed for another 24 h. Next, the solid was filtered and washed with an excess amount of THF and ethanol. Finally, the pale pink solid was dried overnight. Scheme 1 depicts the synthetic procedure of SBA-NCO.

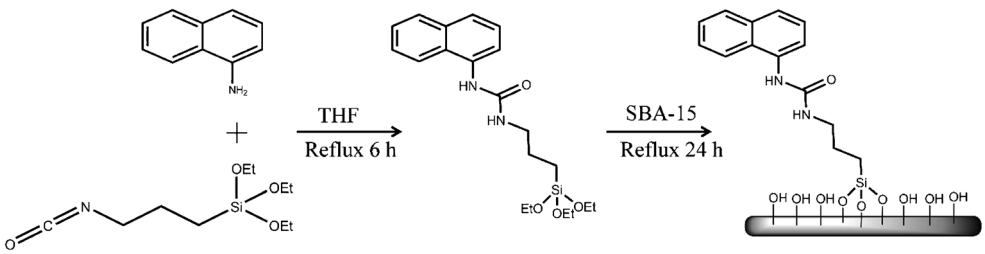

Scheme 1 Synthetic procedure of SBA-NCO

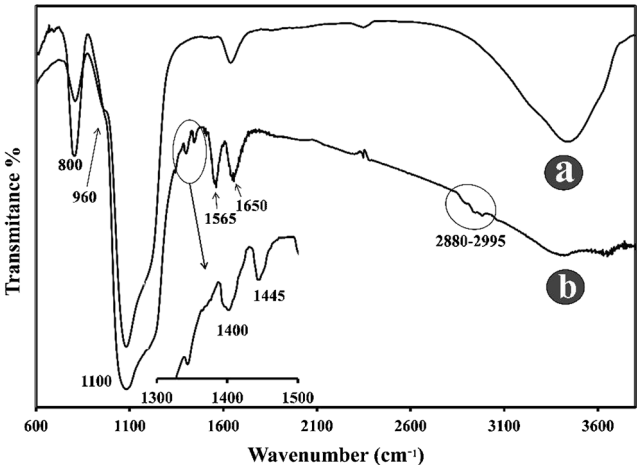

Fig. 2 FT-IR spectra of (a) SBA-15 and (b) SBA-15-NCO

Results and Discussion

Characterizations

The powder XRD patterns of original and functionalized SBA-15 are shown in Fig. 1. All of the materials exhibited the characteristic high intensity peak related to the diffraction from 100 plane near 2θ value of 1°. In addition, they showed two other significant peaks related to the diffraction from 110 to 200 planes near 2θ value of 2° corresponding to the well-ordered one-dimensional hexagonal mesoporous channels of SBA-15. Observing these peaks in SBA-NCO sample indicated that original structure of SBA-15 remained intact after functionalization steps. Nevertheless, lowering the intensity of those diffraction were attributed to decrease in long-range order resulted from grafting of the organic moieties onto the surface of SBA-15. The inset of Fig. 1 shows the TEM image of SBA-15 and the ordered arrays of channels of SBA-15 with pore diameter about 6 nm can be clearly seen which supported XRD result.

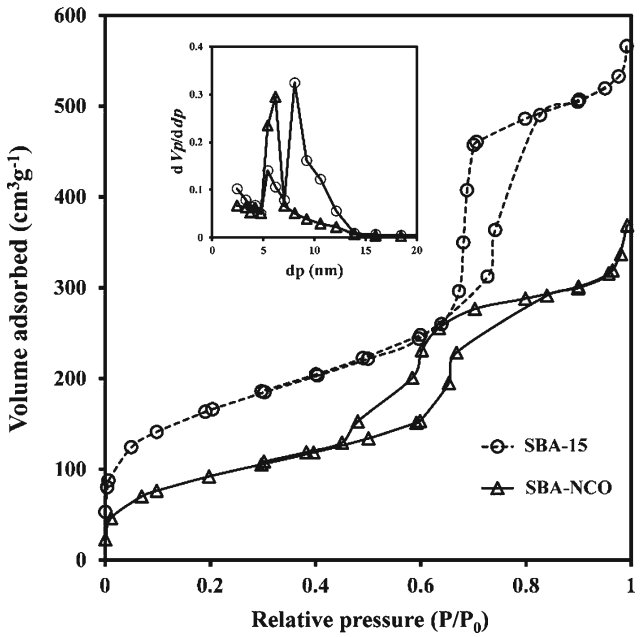

Fig. 3 N_2 adsorption-desorption isotherms of (a) SBA-15 and (B) SBA-NCO

Table 1 Textural properties of SBA-15 and SBA-15-NCO

Sample l	Surface area ($m^2.g^{-1}$)	Pore volume ($cm^3.g^{-1}$)	Average pore diameter (nm)
SBA-15	592	0.87	8.5
SBA-NCO	332	0.56	6.7

The FT-IR spectra of SBA-15 and SBA-NCO are shown in Fig. 2. The wide band around 3360 cm^{-1} in both samples was related to the strong vibration of -OH groups on surface. A series bands within the range of 2880–2960 cm^{-1} were due to the stretching vibrations of methylene -(-CH_2-)- in propyl chain. The bands around 1650 and 1565 cm^{-1} were attributed to the vibrations of physiosorbed water molecules plus C = O stretching vibrations and the bending vibrations of -NH- groups indicating the formation of amide groups. The weak bands around 1400 and 1445 were assigned to the C-N and ring C = C stretching vibrations, respectively. The other remained bands around 800, 960, and 1100 cm^{-1} were attributed to the Si-O-Si symmetric stretching, Si-OH symmetric stretching, and Si-O-Si asymmetric stretching vibrations, respectively. Therefore, the FT-IR results supported the successfully covalent grafting of organic moieties onto the SBA-15 surface.

Textural properties of SBA-15 and SBA-NCO were further investigated using N_2 adsorption-desorption experiment and corresponding isotherms are presented in Fig. 3. Both samples showed type IV isotherms with H1-type hysteresis loops which was characteristic of well-developed uniform

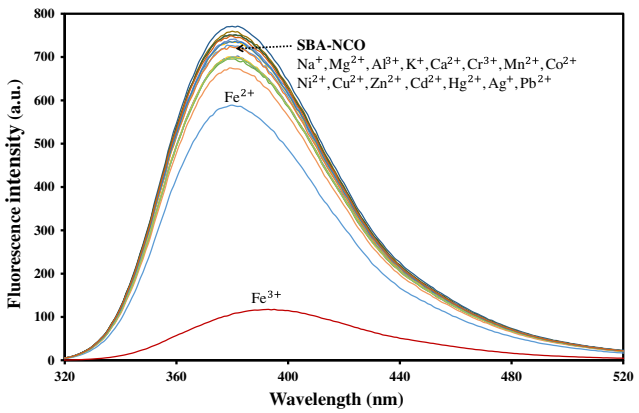

Fig. 4 Fluorescence spectra of the suspended SBA-15-NCO (0.2 $g.L^{-1}$) in the presence of cations (3×10^{-2} M) including Na^+, Mg^{2+}, Al^{3+}, K^+, Ca^{2+}, Cr^{3+}, Mn^{2+}, Fe^{2+}, Fe^{3+}, Co^{2+}, Ni^{2+}, Cu^{2+}, Zn^{2+}, Cd^{2+}, Hg^{2+}, Pb^{2+}

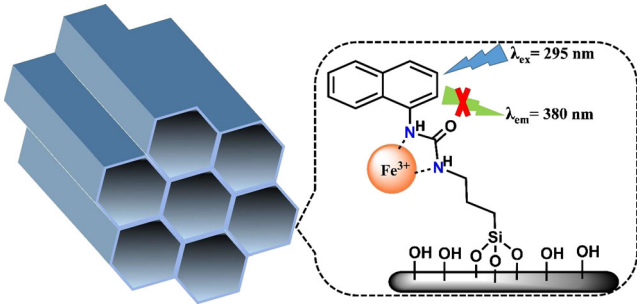

Scheme 2 Binding mode of Fe^{3+}

honeycomb mesoporous materials according to the IUPAC classification [31] confirming XRD results about maintaining mesoporous structure after functionalization step. Decrease in the volume of adsorbed N_2 gas in SBA-NCO was due to the grafted organic moieties onto the SBA-15 surface which consequently led to the reduction of pore sizes, supported by the provided data in Table 1. As expected, the quantity of all three properties in Table 1 were decreased in functionalized SBA-15.

Fluorescence Response of SBA-NCO in Water

In SBA-NCO, urea and naphthalene units acted as a binding site for analytes and fluorophor groups, respectively. In all fluorescence experiments, SBA-NCO was well suspended in water by sonicator to form 0.2 $g.L^{-1}$ monodispersed solution. This suspension was initially tested toward a wide range of metal cations (M^{n+}) including Na^+, Mg^{2+}, Al^{3+}, K^+, Ca^{2+}, Cr^{3+}, Mn^{2+}, Fe^{2+}, Fe^{3+}, Co^{2+}, Ni^{2+}, Cu^{2+}, Zn^{2+}, Cd^{2+}, Hg^{2+}, Pb^{2+}. For this, the fluorescence response of the suspended SBA-NCO (3 ml) in the presence of M^{n+} (3×10^{-4} M) was recorded following excitation at 295 nm with excitation and emission slits of 5 nm. As shown in Fig. 4, SBA-NCO exhibited a strong fluorescence emission with maximum located at 380 nm emitted from naphthalene groups. In the presence of Fe^{2+}, insignificant change in fluorescence intensity was observed, while minimal or no changes were observed for other investigated cations except for Fe^{3+}. As observed in Fig. 4, the fluorescence intensity of SBA-NCO was drastically quenched upon addition of Fe^{3+}. Hence, SBA-NCO exhibited high selectivity for Fe^{3+} over other cations. The quenching effect of Fe^{3+} can be related to the paramagnetic properties of Fe^{3+} ion when it bound to the urea unit (Scheme 2) [32, 33].

For further evaluation of SBA-NCO as a highly selective optical sensor for Fe^{3+}, the competitive experiments were performed in the coexistence of Fe^{3+} and other cations as an interfering ions. The fluorescence spectra were recorded by addition of the suspended SBA-NCO into the mixture of Fe^{3+} (0.5×10^{-4} M)+M^{n+} (2.5×10^{-4} M) following excitation at 295 nm. The derived results in Fig. 5 demonstrated that background metal ions, even with 5 times greater in amount, induced small or no interference with the detection of Fe^{3+} confirming that SBA-NCO is a highly selective optical sensor for Fe^{3+}.

Figure 6 displays the changes in the fluorescence emission of the suspended SBA-NCO (0.2 $g.L^{-1}$) upon addition of an increasing amount of Fe^{3+} following excitation at 290 nm. The amount of Fe^{3+} was varied within the range of 10^{-4}–10^{-6} M. As shown in Fig. 6, upon treatment with Fe^{3+}, a gradual fluorescence quenching was observed, however, the fluorescence intensity was not completely quenched which can be due to the inaccessibility of some fluorophore groups inside the channels. Moreover, the inset of Fig. 6 shows the plot of I_0/I against concentration of Fe^{3+} confirmed good linearity between fluorescence intensity of the suspended SBA-NCO and low-level concentration of Fe^{3+} with r^2=0.9529. As seen in the inset, the deviation from linearity was observed in higher concentrations of Fe^{3+} which could be due to the difficulty of Fe^{3+} ions to reach inner fluorophores. The detection limit (DL) was calculated based on DL=$3S_d/m$ equation, where S_d and m represent standard deviation of the blank solution measured by 6 times and m is the slope of

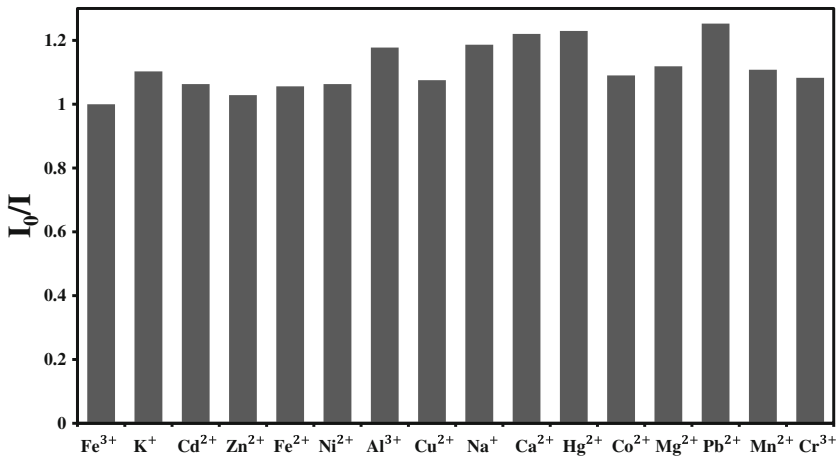

Fig. 5 Normalized fluorescence intensity of the suspended SBA-15-NCO (0.2 $g.L^{-1}$) in the presence of interfering cations (2.5×10^{-4} M) with Fe^{3+} (0.5×10^{-4} M)

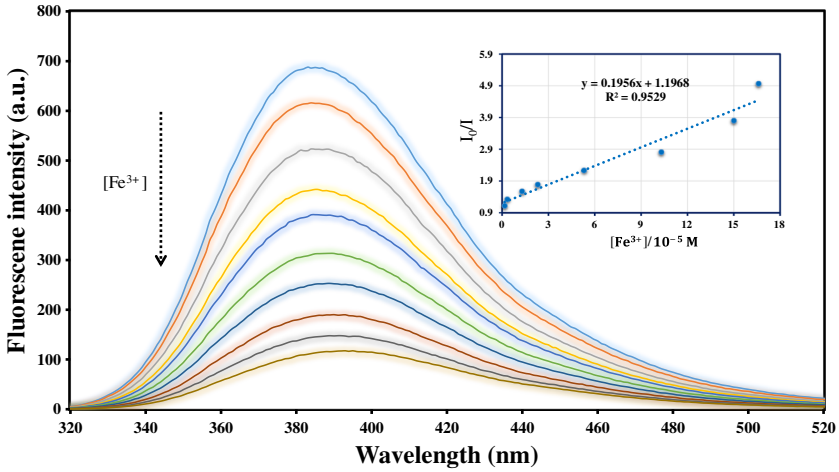

Fig. 6 The fluorescence response of the suspended SBA-15-NCO (0.2 g.L^{-1}) with different concentration of Fe^{3+}. The inset is the Stern-Volmer plot

fluorescence intensity versus concentration of Fe^{3+}. DL was calculated to be 4.5×10^{-6} M.

Practical application of SBA-NCO as a successful optical sensor of Fe^{3+} requires the sensor to be tested in a wide pH range. The fluorescence experiments of the suspended SBA-NCO (0.2 g.L^{-1}) were performed in the absence and presence of Fe^{3+} (3×10^{-4} M) in a pH values ranging from 2 to 12. The pH of the solution was adjusted using either NaOH or HCl solutions. As seen in Fig. 7, the fluorescence intensity of the suspended SBA-NCO were stable and negligibly changed in both mode in the applied pH range. Therefore, the detection of Fe^{3+} using SAB-NCO directly in water was pH independent further confirming SBA-NCO as a successful optical sensor for Fe^{3+} in pure water further.

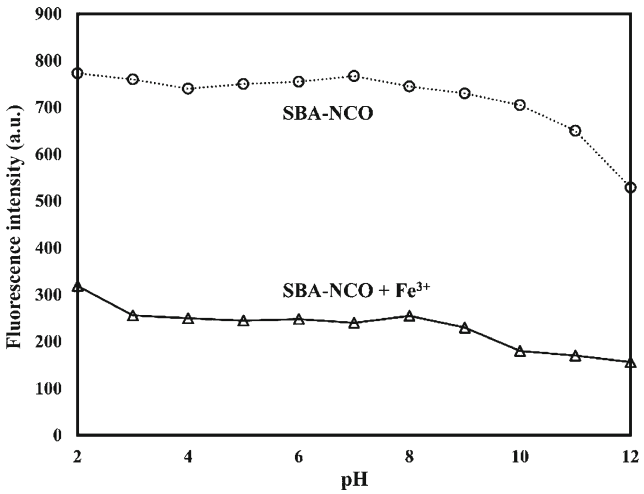

Fig. 7 Effect of the pH on the fluorescence intensity of the suspended SBA-15-NCO (0.2 g.L^{-1}) in the absence and presence of Fe^{3+} (3×10^{-4} M)

Conclusion

In conclusion, a novel organic-inorganic hybrid optical sensor (SBA-NCO) was designed and prepared though functionalization of SBA-15 using isocyanatopropyl-triethoxysilane and 1-amino-naphthalene by post grafting method. The characterization results confirmed the organic moieties were successfully introduced onto the surface of SBA-15 without collapsing in original structure of SBA-15. The fluorescence results displayed that SBA-NCO was a highly selective optical sensor for the detection of Fe^{3+} in pure water without requiring organic solvent even in the presence of higher concentrations of other metal cations as interfering ions and over a wide range of pH values from 2 to 12. Moreover, a good linearity between normalized fluorescence intensity and concentration of Fe^{3+} (r^2=0.9529) with the detection limit of 4.5×10^{-6} M were established.

Acknowledgments The authors thank the research council of University of Tehran for financial support.

References

1. Kim HN, Ren WX, Kim JS, Yoon J (2012) Fluorescent and colorimetric sensors for detection of lead, cadmium, and mercury ions. Chem Soc Rev 41(8):3210–3244
2. Kim HN, Lee MH, Kim HJ, Kim JS, Yoon J (2008) A new trend in rhodamine-based chemosensors: application of spirolactam ring-opening to sensing ions. Chem Soc Rev 37(8):1465–1472
3. Daly B, Ling J, de Silva AP (2015) Current developments in fluorescent PET (photoinduced electron transfer) sensors and switches. Chem Soc Rev 44(13):4203–4211
4. Wenzel M, Hiscock JR, Gale PA (2011) Anion receptor chemistry: highlights from 2010. Chem Soc Rev 41(1):480–520
5. Kumar N, Bhalla V, Kumar M (2014) Resonance energy transfer-based fluorescent probes for Hg 2+, Cu 2+ and Fe 2+/Fe 3+ ions. Analyst 139(3):543–558

6. Sahoo SK, Sharma D, Bera RK, Crisponi G, Callan JF (2012) Iron (iii) selective molecular and supramolecular fluorescent probes. Chem Soc Rev 41(21):7195–7227
7. Papanikolaou G, Pantopoulos K (2005) Iron metabolism and toxicity. Toxicol Appl Pharmacol 202(2):199–211
8. Kabat GC, Rohan TE (2007) Does excess iron play a role in breast carcinogenesis? An unresolved hypothesis. Cancer Causes Control 18(10):1047–1053
9. Jefferies WA, Dickstein DL, Ujiie M (2001) Assessing p97 as an Alzheimer's disease serum biomarker. J Alzheimers Dis 3(3):339–344
10. García-Beltrán O, Mena N, Yañez O, Caballero J, Vargas V, Nuñez MT, Cassels BK (2013) Design, synthesis and cellular dynamics studies in membranes of a new coumarin-based 'turn-off" fluorescent probe selective for Fe 2+. Eur J Med Chem 67:60–63
11. Devaraj S, Y-k T, Chiang C-Y, Yen Y-P (2012) A new dual functional sensor: Highly selective colorimetric chemosensor for Fe 3+ and fluorescent sensor for Mg 2+. Spectrochim Acta A Mol Biomol Spectrosc 96:594–599
12. Bhorge YR, Tsai H-T, Huang K-F, Pape AJ, Janaki SN, Yen Y-P (2014) A new pyrene-based Schiff-base: A selective colorimetric and fluorescent chemosensor for detection of Cu (II) and Fe (III). Spectrochim Acta A Mol Biomol Spectrosc 130:7–12
13. Bao X, Shi J, Nie X, Zhou B, Wang X, Zhang L, Liao H, Pang T (2014) A new Rhodamine B-based 'on-off'chemical sensor with high selectivity and sensitivity toward Fe 3+ and its imaging in living cells. Bioorg Med Chem 22(17):4826–4835
14. Yang M, Sun M, Zhang Z, Wang S (2013) A novel dansyl-based fluorescent probe for highly selective detection of ferric ions. Talanta 105:34–39
15. Yuan A, Zheng C, Zhang Z, Yang L, Liu C, Wang H (2014) A Novel Quinazolinone Derivative as Fluorescence Quenching Off-On Sensor for High Selectivity of Fe3+. J Fluoresc 24(2):557–561
16. Zhang Y, Wang G, Zhang J (2014) Study on a highly selective fluorescent chemosensor for Fe 3+ based on 1, 3, 4-oxadiazole and phosphonic acid. Sensors Actuators B Chem 200:259–268
17. Yin W, Cui H, Yang Z, Li C, She M, Yin B, Li J, Zhao G, Shi Z (2011) Facile synthesis and characterization of rhodamine-based colorimetric and "off–on" fluorescent chemosensor for Fe 3+. Sensors Actuators B Chem 157(2):675–680
18. Chen Y, Jiang J (2013) N, N-di (2-pyridylmethyl) amino-modified porphyrinato zinc complexes. The "ON-OFF" fluorescence sensor for Fe 3+. Spectrochim Acta A Mol Biomol Spectrosc 116:418–423
19. Staneva D, Bosch P, Grabchev I (2012) Ultrasonic synthesis and spectral characterization of a new blue fluorescent dendrimer as highly selective chemosensor for Fe 3+ cations. J Mol Struct 1015:1–5
20. Weerasinghe AJ, Abebe FA, Sinn E (2011) Rhodamine based turn-ON dual sensor for Fe 3+ and Cu 2+. Tetrahedron Lett 52(43):5648–5651
21. Li L, Li L, She N-F, Fei Z, So P-K, Wang Y-Z, Cao L-P, Wu A-X, Yao Z-P (2011) Novel fluorescent molecular clips: selective recognition towards Fe3+ in aqueous solution. J Fluoresc 21(3):1103–1110
22. Zarabadi-Poor P, Badiei A, Yousefi AA, Barroso-Flores J (2013) Selective Optical Sensing of Hg(II) in Aqueous Media by H-Acid/SBA-15: A Combined Experimental and Theoretical Study. J Phys Chem C 117(18):9281–9289, **14**
23. Kim H, Lee S, Lee S, Seo M, Jung J (2008) Reversible solid optical sensor based on acyclic-type receptor immobilized SBA-15 for the highly selective detection and separation of Hg (II) ion in aqueous media. Chem Commun 33:3921–3923
24. Song C, Zhang X, Jia C, Zhou P, Quan X, Duan C (2010) Highly sensitive and selective fluorescence sensor based on functional SBA-15 for detection of Hg 2+ in aqueous media. Talanta 81(1):643–649
25. Zhou P, Meng Q, He G, Wu H, Duan C, Quan X (2009) Highly sensitive fluorescence probe based on functional SBA-15 for selective detection of Hg 2+ in aqueous media. J Environ Monit 11(3):648–653
26. Zhou P, Meng Q, He G, Wu H, Duan C, Quan X (2009) Highly sensitive fluorescence probe based on functional SBA-15 for selective detection of Hg2+ in aqueous media. J Environ Monit 11(3):648–653
27. Meng Q, Zhang X, He C, He G, Zhou P, Duan C (2010) Multifunctional Mesoporous Silica Material Used for Detection and Adsorption of Cu2+ in Aqueous Solution and Biological Applications in vitro and in vivo. Adv Funct Mater 20(12):1903–1909
28. Dong Z, Dong Z, Wang P, Tian X, Geng H, Li R, Ma J (2010) A fluorescent probe for zinc detection based on organically functionalized SBA-15. Appl Surf Sci 257(3):802–806
29. Yadavi M, Badiei A, Ziarani GM (2013) A novel Fe 3+ ions chemosensor by covalent coupling fluorene onto the mono, di- and tri-ammonium functionalized nanoporous silica type SBA-15. Appl Surf Sci 279:121–128
30. Yadavi M, Badiei A (2014) Turn-off Fluorescence Chemosensor for Iron with Bis (2-aminoethyl)-2-(9-fluorenyl) malonamide Functionlized SBA-15. J Fluoresc 24(2):523–531
31. Lee HI, Kim JH, Stucky GD, Shi Y, Pak C, Kim JM (2010) Morphology-selective synthesis of mesoporous SBA-15 particles over micrometer, submicrometer and nanometer scales. J Mater Chem 20(39):8483–8487
32. Tao G-P, Chen Q-Y, Yang X, Wang K-Y (2012) A core-shell silica nanosphere for the off-on chemosensor of iron (III) ions and the targeted probe for optical imaging on HeLa cells. Dyes Pigments 95(2):338–343
33. Xiang Y, Tong A (2006) A new rhodamine-based chemosensor exhibiting selective FeIII-amplified fluorescence. Org Lett 8(8):1549–1552